Journal for ImmunoTherapy of Cancer

Preclinical development of three novel CARs targeting CD79b for the treatment of non-Hodgkin's lymphoma and characterization of the loss of the target antigen

Esperanza Esquinas,[1,2,3] Alvaro Moreno-Sanz,[1] Victor Sandá,[1] Damian Stodulski-Ciesla,[1] Jennifer Borregón,[1] Virginia Peña-Blanque,[4] Javier Fernández-Calles,[5] Narcis Fernandez-Fuentes,[6] Juana Serrano-Lopez,[1,2] Manel Juan ,[7] Pablo Engel,[5] Pilar Llamas-Sillero,[1,2] Laura Solán-Blanco,[1,2] Beatriz Martin-Antonio [1,2,3]

To cite: Esquinas E, Moreno-Sanz A, Sandá V, *et al*. Preclinical development of three novel CARs targeting CD79b for the treatment of non-Hodgkin's lymphoma and characterization of the loss of the target antigen. *Journal for ImmunoTherapy of Cancer* 2024;**12**:e009485. doi:10.1136/jitc-2024-009485

► Additional supplemental material is published online only. To view, please visit the journal online (https://doi.org/10.1136/jitc-2024-009485).

EE and AM-S contributed equally.

Accepted 25 November 2024

For numbered affiliations see end of article.

Correspondence to
Dr Beatriz Martin-Antonio; beatriz.martin@isciii.es

ABSTRACT

Background Infusion of T cells modified with a chimeric antigen receptor (CAR) targeting CD19 has achieved exceptional responses in patients with non-Hodgkin's lymphoma (NHL), which led to the approval of CAR targeting CD19 (CART19) (Axi-cel and Liso-cel) as second line of treatment for adult patients with relapsed/refractory NHL. Unfortunately, 60% of patients still relapse after CART19 due to either a loss of expression of the target antigen (CD19) in the tumor cell, observed in 27% of relapsed patients, a limited CAR-T persistence, and additional mechanisms, including the suppression of the tumor microenvironment. Clinic strategies to prevent target antigen loss include sequential treatment with CARs directed at CD20 or CD22, which have caused loss of the second antigen, suggesting targeting other antigens less prone to disappear. CD79b, expressed in NHL, is a target in patients treated with antibody-drug conjugates (ADC). However, the limited efficacy of ADC suggests that a CAR therapy targeting CD79b might improve results.

Methods We designed three new CARs against CD79b termed CAR for Lymphoma (CARLY)1, 2 and 3. We compared their efficacy, phenotype, and inflammatory profiles with CART19 (ARI0001) and CARTBCMA (ARI0002h), which can treat NHL. We also analyzed the target antigen's expression loss (CD79b, CD19, and B-cell maturation antigen(BCMA)).

Results We found that CARLY2 and CARLY3 had high affinity and specificity towards CD79b on B cells. In vitro, all CAR-T cells had similar anti-NHL efficacy, which was retained in an NHL model of CD19^{-} relapse. In vivo, CARLY3 showed the highest efficacy. Analysis of the loss of the target antigen demonstrated that CARLY cells induced CD79b and CD19 downregulation on NHL cells with concomitant trogocytosis of these antigens to T cells, being most notorious in CARLY2, which had the highest affinity towards CD79b and CD19, and supporting the selection of CARLY3 to design a new treatment for patients with NHL. Finally, we created a CAR treatment based on dual targeting of CD79b and BCMA to avoid losing the target antigen. This treatment showed the highest efficacy and did not cause loss of the target antigen.

Conclusions Based on specificity, efficacy, and loss of the target antigen, CARLY3 represents a potential novel CAR treatment for NHL.

WHAT IS ALREADY KNOWN ON THIS TOPIC

⇒ A proportion of patients with non-Hodgkin's lymphoma (NHL) receiving chimeric antigen receptor (CAR) targeting CD19 (CART19) cells end up relapsing with loss of the target antigen. CD20 and CD22 also cause loss of the target antigen, whereas other antigens, such as B-cell maturation antigen (BCMA), do not cause this event.

WHAT THIS STUDY ADDS

⇒ We develop three novel CARs targeting CD79b and compare their efficacy and loss of the target antigen to that of CARs directed to CD19 and BCMA to select the best candidate to treat patients with NHL who relapse after CART19 with loss of CD19. Moreover, dual CARs targeting CD79b and BCMA emerge as a promising alternative.

HOW THIS STUDY MIGHT AFFECT RESEARCH, PRACTICE OR POLICY

⇒ Results suggest that we could treat patients with NHL who have relapsed to CART19 regardless of the expression of CD19.

INTRODUCTION

Adoptive cellular immunotherapy with autologous T cells modified to express a chimeric antigen receptor (CAR) targeting CD19 (CART19) and B-cell maturation antigen: BCMA (CARTBCMA) has improved the quality of life and the median disease-free

survival of patients with relapsed/refractory (R/R) non-Hodgkin's lymphoma (NHL),[1 2] acute lymphoblastic leukemia[3] and multiple myeloma (MM).[4–6] In NHL, compared with the standard of care (SOC) as second line of treatment, two CART19 products (Axi-cel and Liso-cel) have improved the median disease-free survival (DFS). Specifically, Axi-cel has improved DFS from 8.3 months versus 2.0 months, achieving higher responses (21.5 vs 2.5 months of median DFS at 24.3 months) in older patients (>65 years).[7 8] For Liso-cel, at 17.5 months median follow-up, the median DFS was not reached being of 2.4 months for SOC; and DFS rates at 18 months were 52.6% versus 20.8% for SOC.[9] These results led to the approval of Axi-cel as second line of treatment for adult patients with R/R diffuse large B-cell lymphoma (DLBCL) and high-grade B-cell lymphoma within 12 months after completing the first line of chemoimmunotherapy, and of Liso-cel as second line for treating adult patients with large B-cell lymphoma with early relapse or refractory after first line of chemoimmunotherapy.

However, 60% of patients still relapse after CART19 therapy[7] due to different mechanisms, including a limited persistence of CAR-T cells,[10] which correlates with higher relapse rates and lower progression free sruvival (PFS),[10] and the development of exhaustion in CAR-T cells, among others. Indeed, T cell immunoreceptor with Ig and ITIM domains (TIGIT) and programmed cell death 1 (PD-1) expression predict responses in patients with NHL receiving CART-19 cells,[10] and their combined blockade enhances CART-19 efficacy in patients with NHL.[11] The tumor microenvironment also limits CART cell efficacy through physical barriers and the presence of immunosuppressive cells, such as tumor-associated macrophages,[12] fibroblasts, and vascular endothelial cells[13] that associate with poor response to CART-19 cells in NHL. Of interest, the loss of expression of the target antigen (CD19) in the tumor cell is another relapse mechanism after CART19,[14 15] observed in 27% of relapsed patients.[1] To avoid this issue, it is mandatory to find targets that do not induce loss of expression of the target antigen to obtain durable responses in NHL after CAR-T cell therapy.

Several strategies to prevent the loss of CD19 after CART19 therapy include sequential treatment with CARs directed at CD22 or CD20[16] or treatment with tandem or bicistronic CARs directed at CD19 and CD20 or CD22. These CARs targeting two antigens have demonstrated a lower proportion[17 18] and even a lack of relapses[19] with loss of the target antigen. Of interest, while tandem CARs against CD19 and CD22 have shown only CD19 negative relapses,[20 21] CARs directed at CD19 and CD20 have caused the loss of both antigens,[17] suggesting that some antigens are more prone to disappear than others, such as BCMA, which in patients with MM treated with CART-BCMA, loss of BCMA is hardly observed or only suspected,[22] and preclinical studies have shown that BCMA could be used as a target for NHL.[23] Of interest, targeting CD79b in NHL with polatuzumab vedotin (PV), a CD79b-antibody-drug conjugate, has achieved a lower risk of disease progression, relapse, or death compared with the standard of care with R-CHOP treatment in patients with intermediate-high-risk DLBCL.[24] However, in patients with NHL who relapsed or progressed after CART-19 therapy, PV treatment achieved only short-lived responses as most patients had disease progression,[25] suggesting that CAR-based strategies targeting CD79b will yield better clinical results. Moreover, patients who have lost CD19 after CART19 treatment express CD79b, indicating they could be treated with CD79b-based immunotherapies.

Here, we have developed a new CAR-T therapy for NHL by creating three different CARs against CD79b. These CARs have been termed CARLY (CAR for Lymphoma)1, CARLY2, and CARLY3. We have compared their efficacy, phenotype, and proinflammatory profile among them, and also against CARs directed to CD19 (ARI0001)[26] and BCMA (ARI0002h),[22 27] which are being used to treat patients with NHL and MM. We have also evaluated the loss of expression of the target antigen in models of NHL. All CARLY cells present specificity and anti-NHL activity, with CARLY1 cells showing the lowest efficacy and CARLY3 slight superiority to CARLY2. Importantly, CARLY cells retain their efficacy in an NHL model with a loss of CD19. Regarding the target antigen, whereas CART19 cells cause complete loss of CD19, CARLY cells cause downregulation of both CD79b and CD19 with concomitant trogocytosis of the target antigen to T cells, which was more dramatic for CARLY2 cells. With these results, we have selected CARLY3 as our candidate to treat patients with relapsed NHL to CART19 in a future first-in-human clinical trial that we are preparing. Moreover, to avoid a possible future loss of the target antigen, we designed a dual CAR treatment based on co-transduction with CARLY3 and ARI0002h, showing that this strategy had the highest efficacy and avoided loss of expression of the target antigen.

METHODS

Donors of immune cells

Peripheral blood T cells and monocytes were obtained from buffy coats from healthy donors obtained at "Centro de Transfusiones de Madrid" after obtaining informed consent and being approved by the Centro de Transfusiones de Madrid.

Tumor cell lines

WSU, SC1, and K562 cell lines were purchased from the American Tissue Culture Collection (Manassas, Virginia, USA). Ramos cell line was kindly provided by Juan Manuel Zapata (Instituto de Investigaciones Biomedicas "Alberto Sols", CSIC-UAM, Madrid). The ARP1 cell line was kindly provided by Multiple Myeloma Research Center (Little Rock, Arkansas, USA) under MTA. All tumor cell lines were cultured in RPMI 1640 with 10% fetal bovine serum (FBS) and 1% penicillin/streptomycin (Pen/Strep).

Tumor cell lines were modified to express Green Fluorescent Protine-FireFlyLuciferase (GFP-FFLuc) with lentiviral vectors produced using the plasmids pLV-MSCV_Luc-T2A-GFP (kindly provided by Amer Najjar, MD Anderson Cancer Center, Houston Texas, USA) coding for GFP-FFLuc, and pMD2.G and psPAX2 coding for VSV-G and gag/pol, respectively. *Mycoplasma* testing in cell lines was performed every 2 months.

Production of monoclonal antibodies against CD79b

Balb/c 300.19 mouse cell line was transfected with a chimeric protein composed of the Ig-like domain of CD79b and the second Ig-like domain and transmembrane region of CD84. These cells were used as immunogens in Balb/c mice. Balb/c mice were immunized three times with 30×10^6 cells injected intraperitoneally. After the last immunization, they were fused with the murine myeloma line NS1. Two fusions were made. The first screening was performed by flow cytometry comparing the reactivity of the supernatants using transfected and non-transfected cells. Subsequently, the reactivity of the antibodies (Abs) was validated in peripheral blood cells and CD79b positive and negative cell lines. The selected clones were subcloned by limiting dilution, and their isotype was determined.

Structural modeling of CD79b-CARLY(1,2,3) scFv complexes

The structural models of the CD79b and CARLY 1,2 and 3 single chain variable fragments (scFv) complexes were obtained using data-driven docking as follows. The structure for CD79a in complex with CD79b and IgHM constant mu chain, identification code 7×q8,[28] was taken for the PDB databank.[29] The complementarity-determining regions (CDRs) were defined as defined by the international ImMunoGenetics scheme.[30] The structure of CARLY(1,2,3) scFvs was derived by homology modeling using M4T.[31] The structure of CD79b in complex with CD79a and IgHM constant mu chain was used to identify the epitope of CD79b for docking. The initial docking conformations were inferred using PatchDock[32] by selecting the CDRs of CARLY(1,2,3) scFvs and the predicted epitope of CD79b as docking interfaces. The surface segmentation parameters for CD79b and CARLY(1,2,3) scFvs were set to default except for the *hot spot filter type* which was set to antigen and Ab, respectively. The resulting docking conformation was optimized and minimized using the SnugDock application[33] within the Rosetta suite[34] with default parameters except *refine_outer_cycles*, *max_inner_cycles* and *-h3_filter* set to 2, 20 and true, respectively. Finally, the resulting minimized complexes were sorted by Rosetta global score, and the top 200 poses were visually inspected.

Immunohistochemical analysis

Specificity of the Abs CARLY2 and CARLY3 was analyzed by immunohistochemical analysis using tissue microarrays (TMAs) to facilitate concurrent examination of multiple tissue specimens. This analysis encompassed a comprehensive review of nine TMAs, incorporating a broad array of organ systems. Furthermore, the assessment extended to various lymphoma subtypes, specifically DLBCL, follicular lymphoma, splenic marginal zone lymphoma, marginal zone lymphoma of mucosa-associated lymphoid tissue, and nodal marginal zone B-cell lymphoma, thereby ensuring a wide-ranging investigation of the CAR molecule's antigen specificity across diverse histological context. The immunostaining was executed using an autostainer (Agilent Tech Autostainer Link 48). The TMAs were washed and incubated with a primary Ab solution comprised of supernatant from hybridomes, enriched with CD79b-specific Abs. After another washing step, a secondary reagent containing Mouse+Linker was applied for 15 min to enhance signal amplification. This was followed by applying horseradish peroxidase-conjugated polymer for 20 min. The detection process concluded with applying a substrate-chromogen solution (FLEX DAB+Subchromo) for 10 min, allowing for the visualization of the CD79b antigen signal through staining.

Binding affinity studies

Determination of the binding affinity constant (KD) of Ab/antigen interaction was determined via surface plasmon resonance technology using a Biacore T200. hCD79b was immobilized on a CM5 sensor chip, a glass slide coated with a thin layer of gold. For each sensor chip, one channel was used as a negative control. Each Ab at different concentrations was flown over the CM5 chip and the response was captured over time, showing the progress of the interaction and association/dissociation cycle. After different concentrations were successively tested, the kinetics parameters and affinity were calculated using Biacore software. High affinity Abs are in the low nanomolar range (10^{-9}).

Epitope mapping

The PEPperMAP Epitope Mapping of mAb CD79b.1.50 was performed against CD79B converted into linear 15 amino acid peptides with a peptide-peptide overlap of 14 amino acids for high-resolution epitope data. The resulting CD79B peptide microarrays contained 131 different peptides printed in duplicate (262 spots) (UniProt ID: P40259; aa 29–159). The CD79B peptide microarray was incubated with the Ab at a concentration of 1 µg/mL, followed by staining with secondary (0.2 µg/mL of goat anti-mouse IgG (H+L) DyLight 680) and control Abs. An Innopsys InnoScan 710-IR Microarray Scanner was used to quantify spot intensities and peptide annotation was done with PepSlide Analyzer. Additional details can be found in the online supplemental material.

Lentivirus production for CAR-T cells

All genes coding the different CARLYs were inserted in a pCCL plasmid with EF1a promoter. ARI0001 (from now on ARI1) was provided by Manel Juan (Hospital Clinic of Barcelona), ARI0002h (from now on ARI2h) had been

produced previously by the authors.[26 27] Lentiviral particles were obtained with packaging plasmids pMDLg-pRRE, pRSV-Rev, and envelope plasmid VSV. Production of virus particles to transduce T cells was done in HEK293Tx cells using the same protocol previously described by us, using NaCl, jetPEI, and Lenti-X Concentrator (ClonTech) to collect virus supernatants.[27]

CAR manufacturing

T cells were obtained from buffy coats by Ficoll and magnetic T-cell depletion (Miltenyi Biotec). T cells were expanded in Click's media (47,5% RPMI, 47,5% Click's (Irvine Scientific), 5% human serum, 1% Pen/Strep), activated with Dynabeads Human T-Activator CD3/CD28 (Thermo Fisher Scientific) and IL-2 (100 IU/mL) every other day. After 48 hours of T-cell expansion, viral transduction was performed at an multiplicity of infection (MOI) of 10, and CAR-T cells were left to expand for 7–10 additional days to obtain enough T cells for all in vitro and in vivo studies. T-cell phenotype and experiments were performed at the end of manufacturing.

Macrophage differentiation

After performing Ficoll, monocytes were isolated with RosetteSep Human Monocyte Enrichment Cocktail (STEMCELL Technologies) and macrophages were differentiated from monocytes after 1 week in RPMI 10% FBS and 0.1 mg/mL macrophage colony-stimulating factor (M-CSF) (Thermo Fisher Scientific).

In vivo models

Immunodeficient NSG mice purchased from The Jackson Laboratory. were of the same sex and 8–12 weeks old. Mice were irradiated on day −1 at a dose of 2.5 Gy and received intravenous Ramos-GFP-FFLuc tumor cells on day 0. Depending on the experiment, 7–14 days later, mice received T cells at the dose indicated in each experiment. The disease was followed weekly by bioluminescence. Bone marrow (BM) and spleen were harvested when mice were euthanized to analyze the presence of CAR-T cells and tumor cells by flow cytometry. For survival analysis, mice were euthanized when the bioluminescence signal was higher than 8e10 photons/s, when they lost more than 20% of their weight, or when they presented leg paralysis or ascites.

Cytotoxicity in vitro assays

Luciferase killing assays were performed by co-culturing tumor cells expressing GFP-FFLuc with effector cells in white 96-well plates. D-luciferin (8 µg/mL) was added at the time of plating cells. Bioluminescence was read daily in a Synergy HT Plate Reader (BioTek). The percentage of live tumor cells was calculated as (luminescence of sample/luminescence of tumor cells alone)×100.

Cytokine production

Interferon gamma (IFN-γ), tumor necrosis factor alpha (TNF-α) and interleukin 1-beta (IL-1β) were quantified by ELISA (ELISA Max Deluxe Set, BioLegend) following the manufacturer's protocol.

Confocal microscopy

Ramos, ARP1, and K562 cell lines modified to express GFP were plated in poly-D-lysine-coated slides and stained for CD79b using the monoclonals CB3-1, CARLY2, and CARLY3 in parallel. Anti-mouse IgG-Alexa647 was used as the secondary Ab. Images were acquired using a Leica SP5 microscope. 405, 488, and 633 lasers were used for excitation.

Long-term co-cultures

Ramos-GFP-FFLuc cells were co-cultured with CAR-T cells at an effector:target (E:T) ratio 0.5:1 (2×10^5:4×10^5 cells) in 6-well plates, adding 4 mL of total media to hinder the access of CAR-T cells to tumor cells. These conditions enabled a slow killing that would provide enough time to make easier the development of tumor antigen loss. As tumor cells had GFP-FFLuc, every day, bioluminescence and fluorescence were read to assess tumor cell survival. Fluorescence was also evaluated by microscopy to check tumor-CAR-T cell clusters (online supplemental figure 6A) which are required for CAR-T cells to kill. However, when GFP clusters were stable for 2–3 days and bioluminescence continued to grow, meaning that CAR-T cells were still there but stopped the killing, a timing that varied between experiments, the expression of the target antigen was analyzed by flow cytometry.

Flow cytometry

CAR expression for ARI2h was detected with a recombinant BCMA-Fc protein (Enzo Life Sciences). For the other CARs, a Biotin-SP AffiniPure Goat Anti-Mouse IgG, *F*(ab')$_2$ (Jackson ImmunoResearch), and Streptavidin Super Bright 436 Conjugate (Thermo Fisher Scientific) were used. For CARLY2 and 3 affinities towards cell lines, a secondary Anti-mouse IgG, *F*(ab')$_2$ Alexa Fluor-647, was added after incubating with CARLY2 and 3. For T-cell phenotyping, PD-1-APC (clone: J105), TIM-3-FITC (clone: F38-2E2), TIGIT-PerCP-Cy5.5 (clone: A15153G), LAG-3-PE (clone: 11C3C65), CXCR3-Alexa Fluor 488 (Clone 1C6/CXCR3), CCR7-PerCP-Cy5.5 (clone: 150503), CD45RA-APC (clone: HI100), CD27-PE (clone: M-T271), CD28-FITC (Clone CD28.2), CD3-PE (clone SK7), CD4-APC-H7 (clone L200) and CD8-PE-Cy7 (clone: RPA-T8) Abs were used. CD79b-PE (clone CB3-1), CD19-Percp-Cy5.5 (cloneHIB19) and BCMA-Alexa-647 (clone 19F2) were used to analyze the loss of the target antigen. For T-cell determination in BM or spleen at in vivo endpoint, mouse FcR blocking reagent (Miltenyi) was used. All experiments were read on an FACSCanto II (BD Biosciences) and analyzed with FlowJo software (Tree Star, Eugene, Oregon, USA).

Graphs and statistical analysis

Data and statistical analysis were presented and performed using GraphPad Prism software V.8.0.1. Analysis of variance test was conducted to compare between groups.

RESULTS

The scFvs coding for CARLY1 and CARLY2 have higher homologies being CARLY3 the most different

The three new monoclonal murine Abs produced against CD79b were named CARLY (CAR for Lymphoma)1, 2 and 3. The reactivity of the three hybridoma supernatants against NHL (Ramos and Daudi) cell lines was confirmed by flow cytometry (figure 1A). In parallel, NHL (Ramos, SC1, and WSU) and MM (ARP1 and U266) cell lines used for all in vitro studies were stained with commercial anti-CD79b (CB3-1 clone) and BCMA (clone 19F2) Abs. NHL cells presented high CD79b and low BCMA staining, and MM cell lines showed high BCMA levels and almost undetectable staining for CD79b (figure 1B). Measurement of the number of CD79b, CD19 and BCMA molecules on the membrane with commercial clones (CB3-1, HIB19 and 19F2) confirmed that NHL cells (Ramos, WSU, and SC1) had a very high number of CD79b and CD19 molecules on the cell membrane and extremely low BCMA levels, and MM cell lines presented a high number of BCMA molecules on the membrane although non-detectable levels of CD79b and CD19 (figure 1C).

CARLY1, 2, and 3 scFvs were sequenced to design three second generation CAR-T cells with 4-1BB co-stimulatory domain and CD8a hinge and transmembrane domains (figure 1D). Amino acid sequence alignment of the three scFvs showed that compared with CARLY1, CARLY3 was the most different in both the heavy and light chains. This higher disparity for CARLY3 was maintained in the CDRs responsible for recognizing the tumor epitope (figure 1E–1F). We performed structural predictive models of the different scFvs complexes bound to CD79b to have additional information. Some structural differences in the location of the CDRs and the exposed area of the scFvs complexed with CD79b and with IgH constant mu were observed (figure 1G and H).

CARLY2 and CARLY3 have high specificity in recognizing NHL cells

Of the three hybridomes, only the Abs for CARLY2 and 3 could be purified, which we used to perform affinity binding studies towards human CD79b and to analyze their specificity towards NHL cells and other types of cells. CARLY2 and 3 had an equilibrium dissociation constant (KD) in the nanomolar range, indicating strong affinity with human CD79b and showing CARLY2 a higher binding affinity (figure 2A). This higher affinity was confirmed after staining NHL cell lines (figure 2B,C). Moreover, CARLY2 and CARLY3 reactivity were compared by confocal fluorescence microscopy towards the CB3-1 clone, showing that they all stained Ramos cell line with a membrane pattern and that CB3-1 also stained ARP1 MM cell line with a membrane pattern and also K562 cells slightly with unspecific pattern (figure 2D), indicating the high specificity of CARLY2 and CARLY3 towards NHL cells. In addition, we stained formalin-fixed paraffin-embedded tissue samples of patient with different healthy tissues and NHL samples using CARLY2 to find out the possible on-target, off-tumor toxicity that CARLY cells could have. CARLY2 stained the positive controls (Tonsil) and different NHL samples. No staining was observed in other healthy tissues (brain, heart, and stomach), and some staining corresponding to B cells in BM and the gut was detected (figure 2E).

Although patients receiving CAR-T cells present cytopenia[6] due to previous chemotherapy and lymphodepletive conditioning regimens, we analyzed whether CARLY cells could also induce neutropenia. We analyzed the recognition of peripheral blood mononuclear cells and CD34 on BM samples by CARLY2 and 3. CARLY2 and 3 only stained the lymphocyte subset (figure 2F,G). Finally, staining of tumor cell lines representative of other tissues (breast, fibroblasts, prostate, colon, neuronal cells) confirmed the lack of reactivity of CARLY2 and 3 (figure 2H).

Manufacturing of CARLY1, 2, and 3 does not provide products with high differences in the T-cell phenotype

Once we had confirmed the specificity of our CARs, we compared whether manufacturing the different CAR-T cells would lead to differences in the final product. We compared the three CARLY cells with untransduced (UT) T cells, and also with CART19 (ARI0001: ARI1) and CARTBCMA (ARI0002h: ARI2h) cells that were used for all efficacy studies. For all CARs, the efficacy of CAR transduction was higher than 60% (figure 3A). The CD4 and CD8 T-cell proportions did not vary significantly between the different CARs. However, in the final product, CAR^+ T cells contained a higher proportion of CD4 T cells than CAR^- T cells (figure 3B). We analyzed the ratio of cells showing Th17 (CD4+, CCR6+CCR4+) phenotype among the CD4 population. The number of T cells showing Th17 phenotype did not vary from day 0 and remained at a low profile, hovering around 5% of the cells analyzed (figure 3C).

Analysis of the differentiation stage of T cells determined by using CCR7, CD45RA and CXCR3 markers showed high variability between the different donors but no high differences among the different CARs. As expected, naïve and stem cell memory (SCM) T cells decreased significantly after CAR manufacturing for all groups of CD4 and CD8 T cells, as they differentiated into central memory (CM) and effector memory T-cell subsets (figure 3D–3F). For CD8 CAR+T cells, CARLY1, which showed the highest loss of naïve/SCM, presented with the highest proportion of CM T cells (figure 3E). Moreover, CARLY1 and 2 had a lower proportion of terminally differentiated CD8 T cells than UT T cells (figure 3E).

Senescent T cells can be defined by a loss of CD28 and CD27 costimulatory molecules and the acquisition of CD57 and KLRG1. Increasing cell size might also indicate senescent stages.[35] No differences were observed in cell size among the different groups of CAR-T cells after manufacturing (figure 3G). Of interest, on day 0, there was a higher proportion of CD8 senescent T cells than CD4 T cells, which dropped significantly to less than 1%

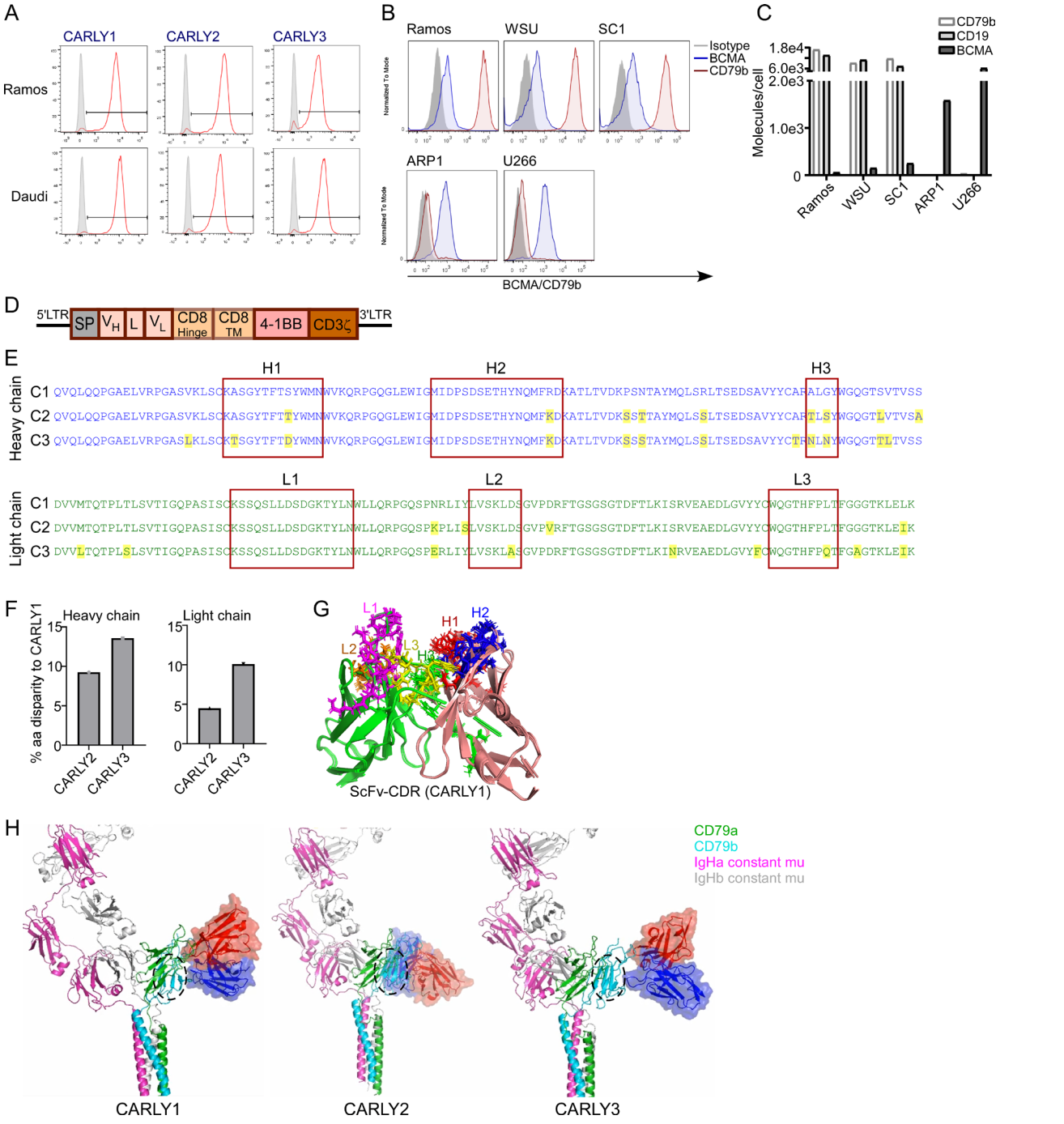

Figure 1 Specificity of three new antibodies targeting CD79b to design three new CARs. (A) Flow cytometry staining of B-cell lines (Ramos and Daudi) using the hybridoma supernatants obtained after production of CARLY1, 2, and 3. (B) CD79b and BCMA expression in NHL (Ramos, WSU, SC1) and MM (ARP1, U266) cell lines using commercial monoclonals against CD79b (CB3-1 clone) and BCMA (19F2). (C) Quantification of the number of CD79b, CD19, and BCMA molecules on the surface of NHL and MM cell lines using commercial antibodies (CB3-1, HIB19 and 19F2 clones). (D) Design of the CAR construct of CARLY1, CARLY2 and CARLY3 showing the signal peptide, variable heavy chain (VH), linker (L) and variable light chain (VL), CD8 hinge and transmembrane domains, 4-1BB costimulatory and CD3ζ activation domains. (E) Amino acid (aa) sequence of the VH and VL for CARLY1, 2 and 3 (C1, C2, C3). Differences of CARLY2 and CARLY3 compared with CARLY1 are highlighted in yellow. The complementarity determining regions (CDR) for the VH (H1, H2, H3) and VL (L1, L2 and L3) chains that recognize CD79b are shown in enclosing rectangles. (F) Percentage of aa homology of CARLY2 and 3 compared with CARLY1 for the variable heavy and light chains. (G) 3D model of the scFv coding for CARLY1, showing the structural location of the CDRs of the VH (H1, H2, H3) and VL (L1, L2, L3) chains. (H) 3D docking models showing cryo-EM structure of heterodimers CD79a/b chains and IgH constant mu chains bound to the different scFvs (CARLY1, 2 and 3). Indicated in the black dashed circle is the epitope region of CD79b used to dock the different CARLYs and derive the structural complexes. BCMA, B-cell maturation antigen; CAR, chimeric antigen receptor; CARLY, CAR for Lymphoma; MM, multiple myeloma; NHL, non-Hodgkin's lymphoma; scFV, Single chain variable fragment; 3D, three-dimensional.

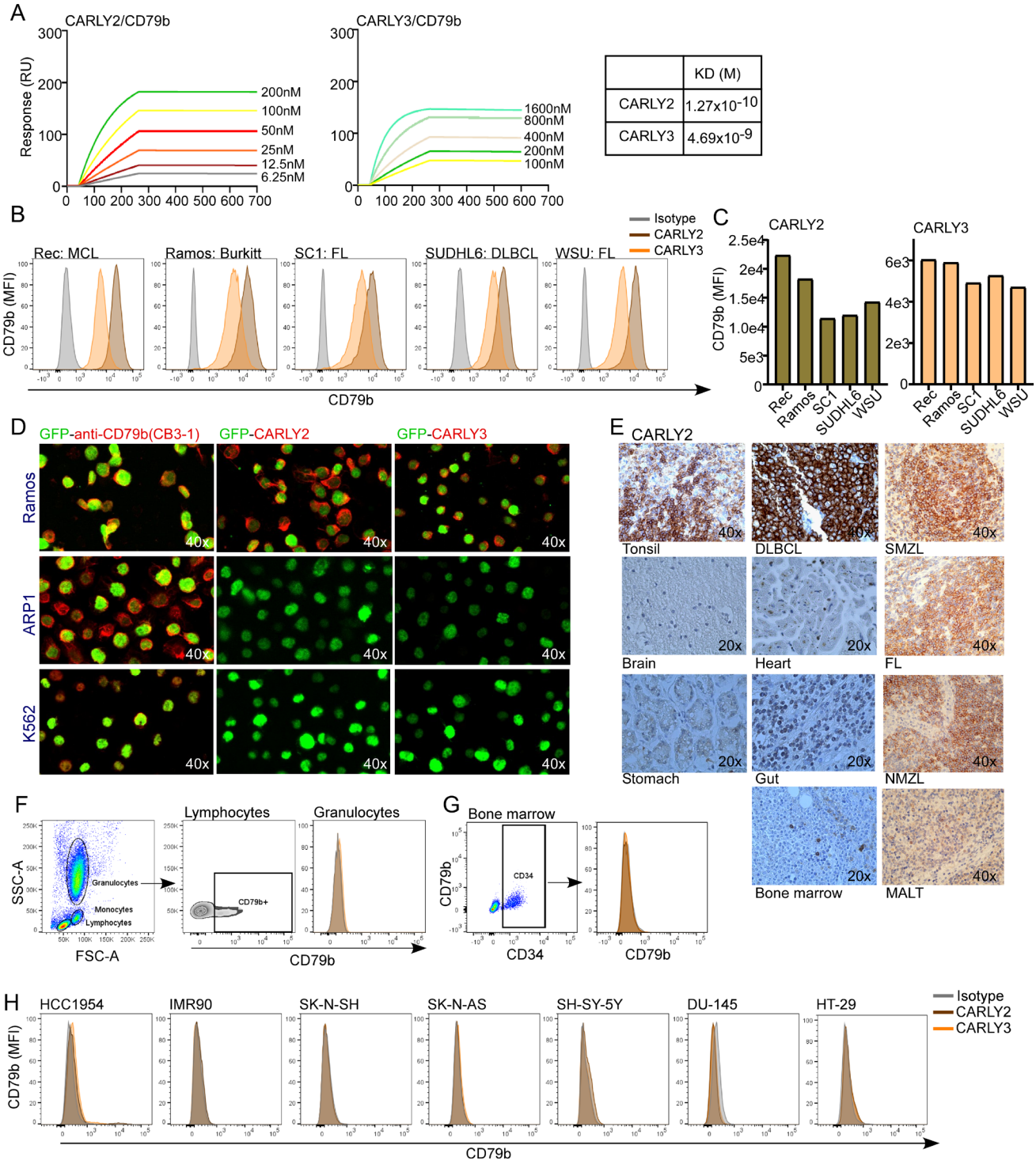

Figure 2 Binding affinity and specificity of CARLY2 and 3 towards CD79b. (A) Binding affinity assays of CARLY2 and 3 towards CD79b antigen performed at different concentrations of CD79b indicating the equilibrium dissociation constant values obtained (KD). (B–C) Flow cytometry staining of cell lines representative of different types of NHL using CARLY2 and CARLY3. (D) Staining in NHL cells (Ramos), multiple myeloma cells (ARP1) and a negative control (K562) using a commercial anti-CD79b (clone CB3-1), CARLY2 and CARLY3. Cell lines express GFP (green), and CD79b is shown in red. (E) Paraffin-embedded tissues stained with CARLY2 of different tissues and different types of NHL (SMZL, FL, NMZL, MALT). Tonsil was used as a positive control. (F–G) Reactivity of CARLY2 and 3 in peripheral blood mononuclear cells (F) and bone marrow (G) of healthy donors showing recognition of lymphocytes, and not of granulocytes and CD34+cells. (H) Reactivity of CARLY2 and CARLY3 in cell lines representative of other solid tissues. HCC1954: epithelial breast cancer. IMR90: lung fibroblast. DU-145: prostate cancer. HT-29: colon adenocarcinoma. SK-N-SH, SK-N-AS and SH-SY-5Y are neuroblastoma cell lines. See also online supplemental figure 2. CARLY, chimeric antigen receptor for Lymphoma; DLBCL, diffuse large B-cell lymphoma; FL, follicular lymphoma; GFP, green fluorescent protein; MALT, mucosa-associated lymphoid tissue; MCL, mantle cell lymphoma; MFI, median fluorescence intensity; NHL, non-Hodgkin's lymphoma; NMZL, nodal marginal zone lymphoma; SMZL, splenic marginal zone lymphoma.

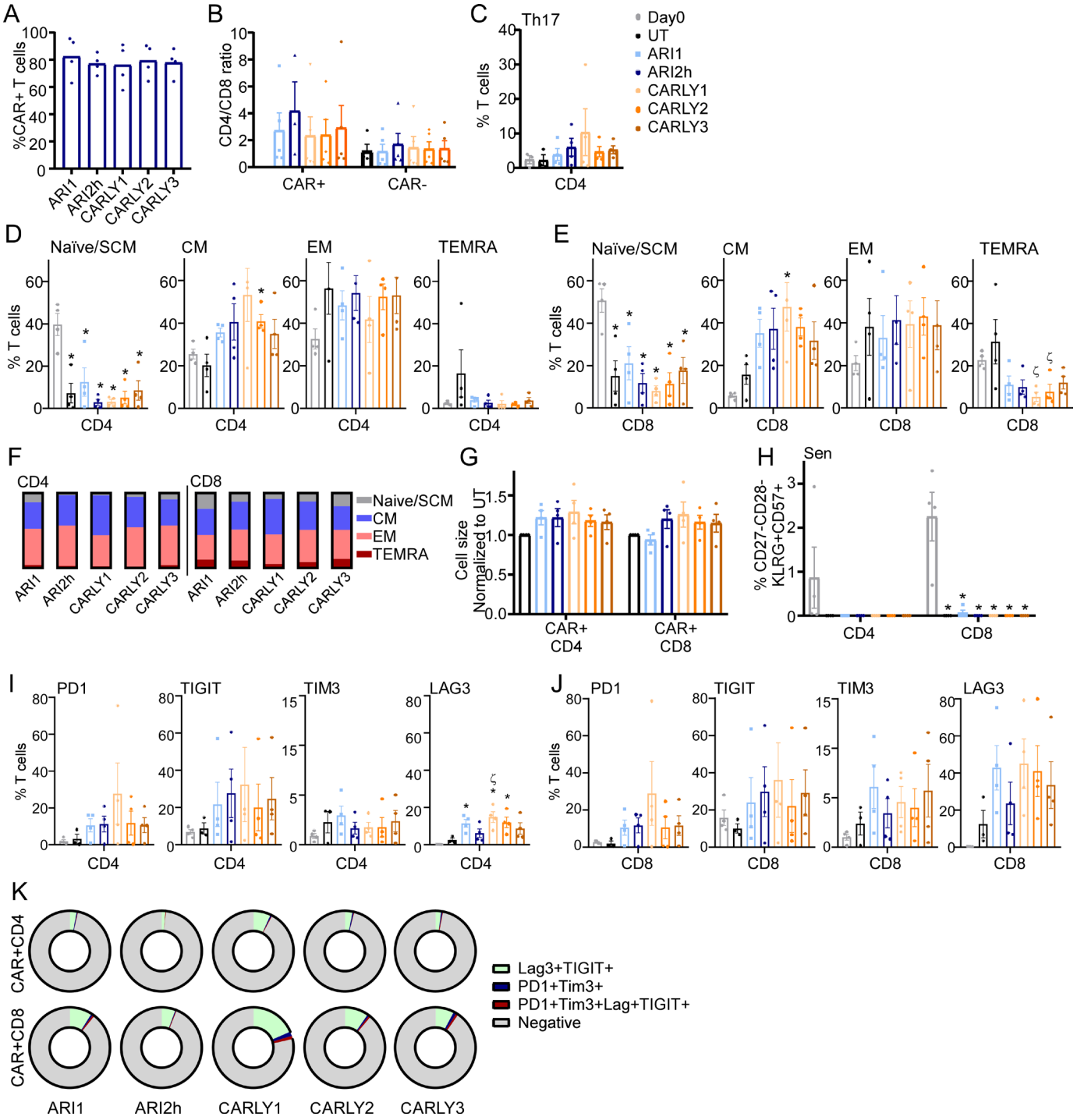

Figure 3 Phenotypic characterization of CARLY1, 2, and 3 compared with CAR targeting CD19 (ARI1), and CARTBCMA (ARI2h) cells after their production. (A) Percentage of CAR+cells obtained after T-cell transduction and after 7 days of expansion of the different CARs. (B–K) Characterization of the different CAR products after 7 days of expansion of five different donors. Values at day 0 before CAR transduction are shown. (B) CD4/CD8 ratio in the CAR+ and CAR-fraction. (C) Th17 proportion in the CD4 T-cell subsets. (D–F) Memory T-cell differentiation stages (naïve, stem cell memory (SCM), central memory (CM), effector memory (EM) terminally differentiated (TEMRA) T cells in CD4 (D) and CD8 (E) are shown. (G–H) T-cell size (G) and proportion of senescent CAR+T cells (H) defined as $CD27^{-}CD28^{-}KLRG^{+}CD57^{+}$. (I–K) Expression of markers related to exhaustion in CD4 (I) and CD8 (J) CAR+T cells. (K) Co-expression of different exhaustion markers in a representative CAR-T production with the different CARs. In (C–J) statistics were performed comparing versus day 0 (*p<0.05) and versus UT T cells (ζ:p<0.05). See also online supplemental figure 3. BCMA, B-cell maturation antigen; CAR, chimeric antigen receptor; CARLY, CAR for Lymphoma; Lag3, Lymphocyte activating 3; PD-1, programmed cell death 1; TIGIT, T cell immunoreceptor with Ig and ITIM domains; Tim3, T cell immunoglobulin mucin; UT, untransduced.

in all CAR groups following CAR manufacturing and showed no differences in the different T-cell products (figure 3H).

The analysis of T-cell exhaustion did not show differences between the different CARs for PD-1, TIGIT and T cell immunoglobulin mucin (Tim3) (figure 3I and J). Despite the variability among different donors, compared with day 0, CD4 Lag3+T cells increased in CARLY1, CARLY2, and ARI1 cells. CARLY1 also had a higher proportion of CD4 Lag3+T cells than UT T cells after manufacturing (figure 3I). We noticed that some individual exhaustion markers were expressed at high levels, which could reflect an activation status of T cells after the manufacturing. Therefore, we analyzed the co-expression of either two or four exhaustion markers, showing that the co-expression of lymphocyte activating 3 (Lag3) and TIGIT was higher, especially for CARLY1. However, co-expression of the four markers was barely detectable, indicating that CAR-T cells were not exhausted after the manufacturing (figure 3K and online supplemental figure 3).

All CARLY cells present comparable anti-NHL in vitro efficacy compared with ARI1 or ARI2h cells and retain their efficacy in an NHL model with loss of CD19.

The anti-NHL activity of the different CARLY cells was compared with that of UT-T cells, ARI1, and ARI2h cells. Cytotoxicity assays at different E:T ratios showed that, as expected, all CARs killed NHL cells (Ramos and WSU) with high efficacy at 1:1 and 0:25:1 E:T ratio (figure 4A–4B). As ARP1 MM cells do not express CD19 and CD79b antigens, they were only eliminated by ARI2h cells. However, at 1:1 ratio, we observed some ARP1 killing by CARLY1 cells, although this killing was lost when we lowered the ratio (figure 4C). No killing was observed for any CAR-T against the K562 line, used as a negative control (figure 4D).

The pro-inflammatory profile of each CAR was compared in these assays by analyzing cytokine production after co-culture with NHL Ramos cells in the presence/absence of macrophages. As expected IFN-γ and TNF-α production was higher in the presence of macrophages, and IL-1β could only be detected in the presence of macrophages (figure 4E). ARI1 cells showed the lowest cytokine release. In macrophage-free, the three CARLYs had similar and higher IFN-γ production than the other CAR-Ts. TNF-α production usually occurs very fast and decays over time.[27] Without macrophages, we confirmed this TNF-α pattern for all CARs but for CARLY3, whose production started later and was still increasing at 48 hours. In the presence of macrophages, CARLY2 and 3 showed the same trend, which might indicate either a slower kinetics or a higher pro-inflammatory profile. IL-1β, as expected, was not detected in the absence of macrophages, and with macrophages, ARI1 and CARLY1 induced the lowest IL-1β production (figure 4E).

Moreover, to mimic a model of CD19$^-$ relapse, we exposed the different CARs to NHL Ramos cells where CD19 was removed by CRISPR-Cas9 (Ramos 19-KO). As expected, UT T and ARI1 cells did not eliminate NHL cells, whereas all CARLY cells and ARI2h cells killed them at different E:T ratios (figure 4F).

Among the three CARLYs, CARLY1 has the lowest and CARLY3 the highest in vivo efficacy in a model of NHL

The anti-NHL activity of all CARs was compared in vivo in a model of NHL where mice received CAR-T cells 7 days after the NHL cells (figure 5A). Mice treated with UT T cells could not avoid disease progression, whereas all CAR-T cells delayed disease progression, being CARLY2, CARLY3, and ARI2h, the groups showing the highest differences compared with UT T cells (figure 5B–D). All CAR groups achieved a higher survival rate than UT T cells. However, it was only significant for mice treated with CARLY2 and CARLY3, where CARLY3 had the most prolonged survival and CARLY1 the shortest (figure 5D).

At the final point, flow cytometry analysis of GFP+tumor cells confirmed that UT mice had the highest engraftment of tumor cells in BM and spleen, being more abundant in the spleen than in BM (figure 5E). Analysis of the different treatments showed that CARLY1 and ARI1 conferred worse protection than CARLY2, CARLY3 and ARI2h. Specifically, ARI1 and CARLY1 showed similar tumor engraftment to UT T cells in BM, showing this pattern also CARLY1 in the spleen (figure 5E). Analysis of CD3 T cells on the surviving mice on day 40 indicated that they were present in a very low percentage for all groups of CARs, and even though some differences were observed, these were not significant (figure 5F). In addition, we observed that when the disease was out of control, mice developed splenomegaly that correlated with the presence of tumor cells in the spleen (figure 5G).

Last, we analyzed the expression of the target antigen (CD79b, CD19 and BCMA) in tumor cells. Considering the low number of samples with enough tumor cells to analyze, no significant findings were observed (figure 5H). However, we noticed that in mice treated with CARLY1 where the disease progressed at late time points (late relapse), there was a downregulation of CD79b, and also a decrease in CD19 and BCMA was observed, a finding not observed in cases where the disease progressed initially (no response) (figure 5I–5J). Furthermore, in cases of late relapse for CARLY3, downregulation of CD79b was also observed (online supplemental figure 5A)

Further in vivo comparison of the three CARLYs with another NHL cell line (WSU) confirmed the highest survival conferred by CARLY3 compared with CARLY1, and mice treated with CARLY2 and CARLY3 had the highest number of T cells in BM (online supplemental figure 5B–G). Of note, downregulation of the target antigen was also detected in this experiment but not a complete loss (online supplemental figure 5H).

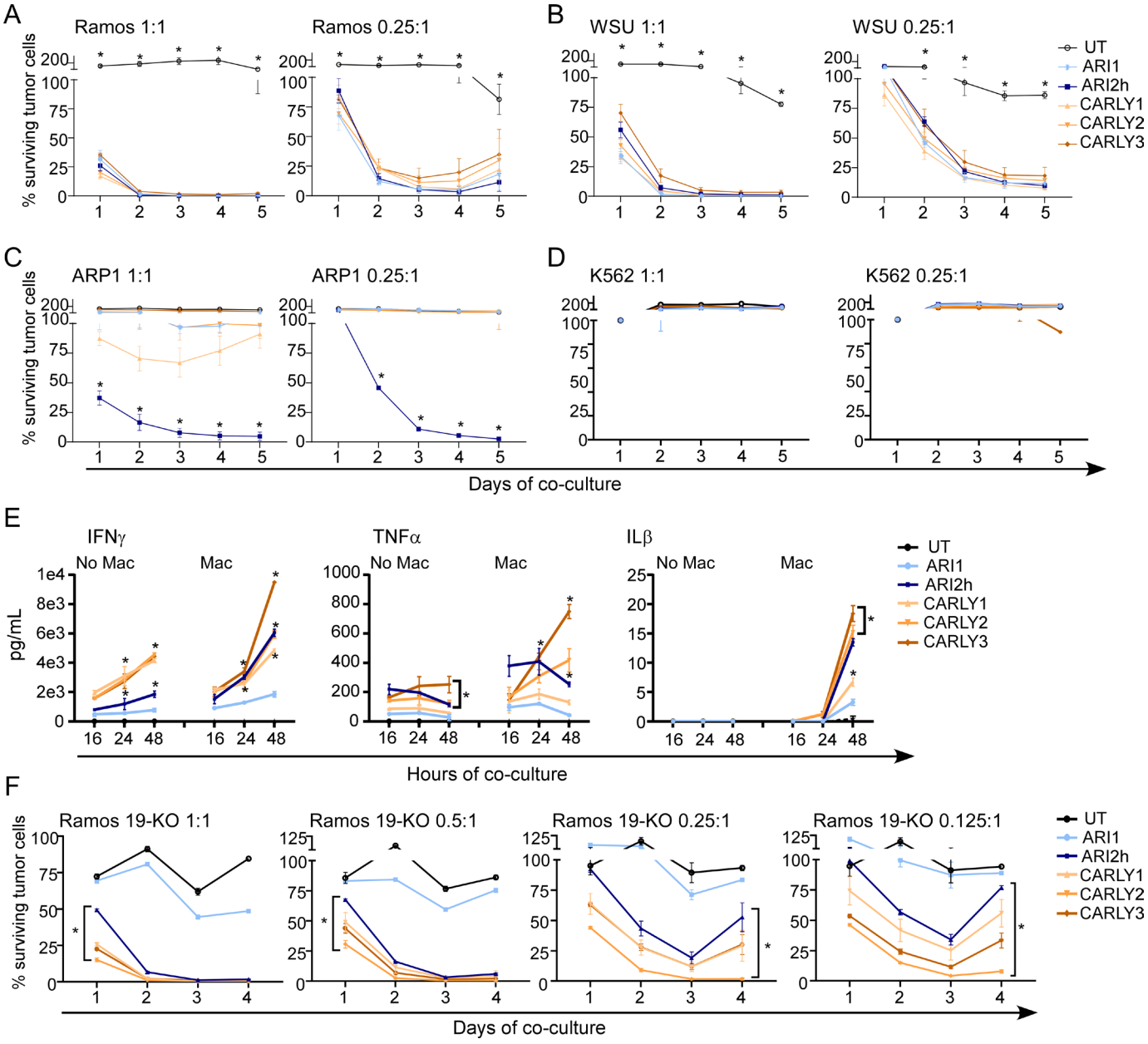

Figure 4 Anti-NHL in vitro activity and inflammatory profile of CARLY cells compared with ARI1 or ARI2h cells: (A–D) in vitro cytotoxicity assays of the different types of T cells (untransduced: UT, and the different CAR-T cells) co-cultured with NHL (Ramos and WSU) cells (A and B), MM-ARP1 cells (C) and K562 (D) cells used as negative control. Assays were performed at different effector:target (E:T) ratios. (E) IFN-γ, TNF-α and IL-1β production after co-culturing Ramos cells with the different CARs in the presence/absence of macrophages (Mac) at 0.5:1 E:T ratios adding half proportion of Mac compared with T cells. (F) In vitro cytotoxicity assays of the different types of T cells in a model of NHL-Ramos cells with loss of CD19 (19-KO). In (A–E) statistics were performed comparing versus UT and in (F) versus ARI1 cells (*p<0.05). Results were confirmed at least in three different donors. CAR, chimeric antigen receptor; CARLY, CAR for Lymphoma; IFN, interferon; IL, interleukin; NHL, non-Hodgkin's lymphoma; TNF, tumor necrosis factor.

CARLY cells cause downregulation of the target antigen in NHL cells concomitant with trogocytosis of the antigen from tumor cells to CAR-T cells

As in vivo data suggested downregulation of the target antigen, we analyzed in vitro loss of expression of the target antigen (CD79b, CD19, and BCMA) in culture conditions where CAR-T cells made stable co-cultures with tumor cells and stopped their killing (figure 6A, online supplemental figure 6A). We added a new condition using a dual CAR targeting BCMA and CD79b to determine whether this approach would prevent this issue. This dual CAR was achieved by co-transduction of T cells with CARLY3 and ARI2h lentiviral particles. Co-transduction efficiency showed that T cells could express both CARs together, and that single CARLY3 cells were at a lower proportion than single ARI2h cells (figure 6B). The target antigen was analyzed in both tumor cells and T cells at these co-co-cultures (figure 6C). We confirmed

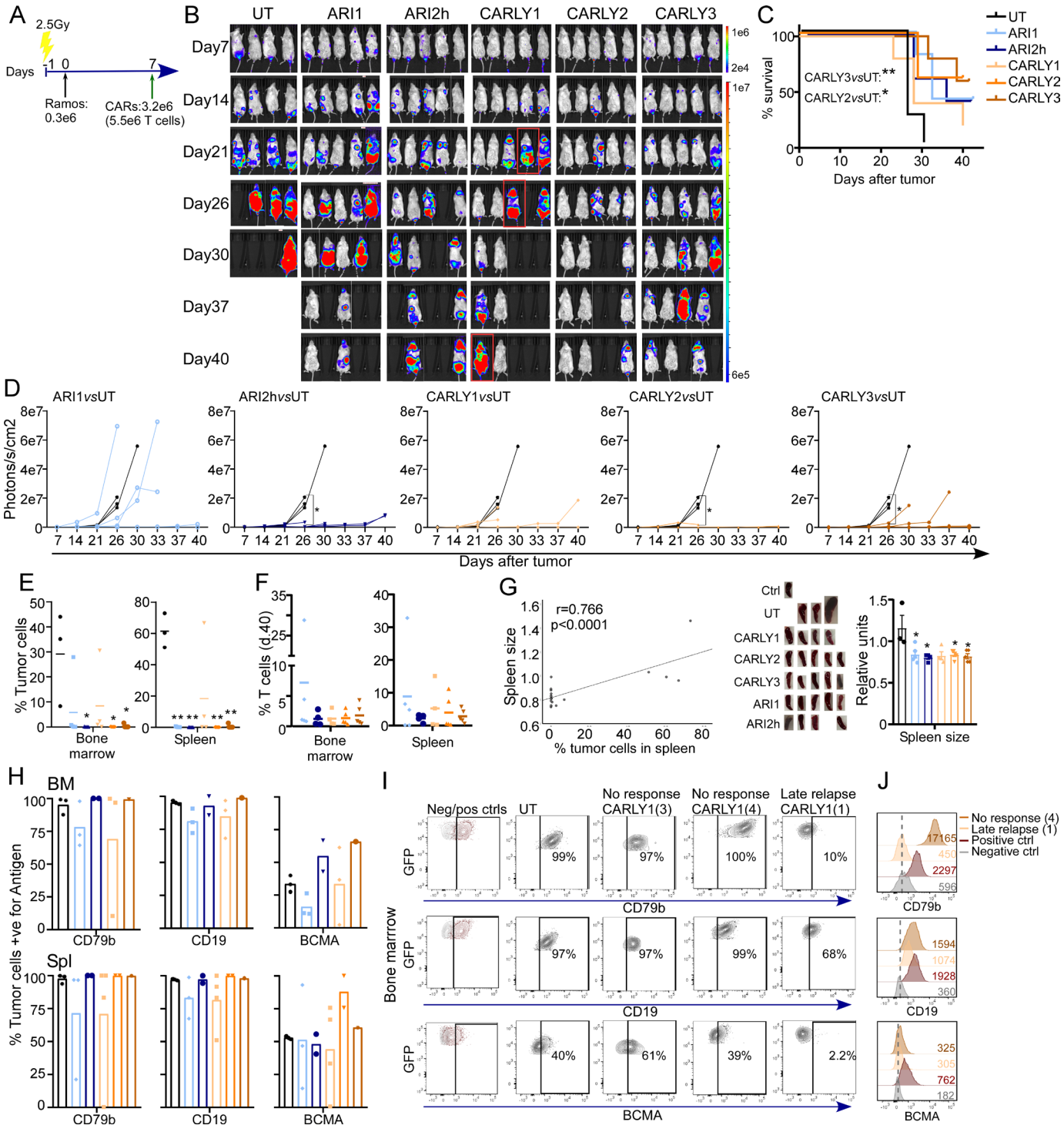

Figure 5 In vivo efficacy of the different CARLY cells compared with ARI1 or ARI2h cells. (A) Timing and doses of cells that mice received. (B–C) Disease progression is followed weekly by bioluminescence. (C) Represents numerical luminescence values of images in (B, D). Mice survival of the different groups. (E–F) Percentage of tumor cells (E) and of T cells at final point (F) in bone marrow and spleen. (G) Correlation analysis of the size of spleens with the percentage of tumor cells in the spleen of the different mice. Spleens are shown in the photo. (H–J) Analysis of expression of the target antigen (CD79b, CD19 and BCMA) in tumor cells in bone marrow (BM) and spleen (Spl). (H) Shows the percentage of tumor cells indicating at the left negative and positive controls used to do the gates. (I) Shows the flow cytometry plots of mice treated with either UT T or CARLY1 cells, comparing mice where disease progressed quickly (no response, mice 3 and 4) and mice where disease progressed later (late relapse, mouse 1). (J) MFI values of mice shown in (I) for each antigen. *p<0.05 compared with UT T cells. See also online supplemental figure 5. BCMA, B-cell maturation antigen; CAR, chimeric antigen receptor; CARLY, CAR for Lymphoma; MFI, Median Fluorescence Intensity; UT, untransduced.

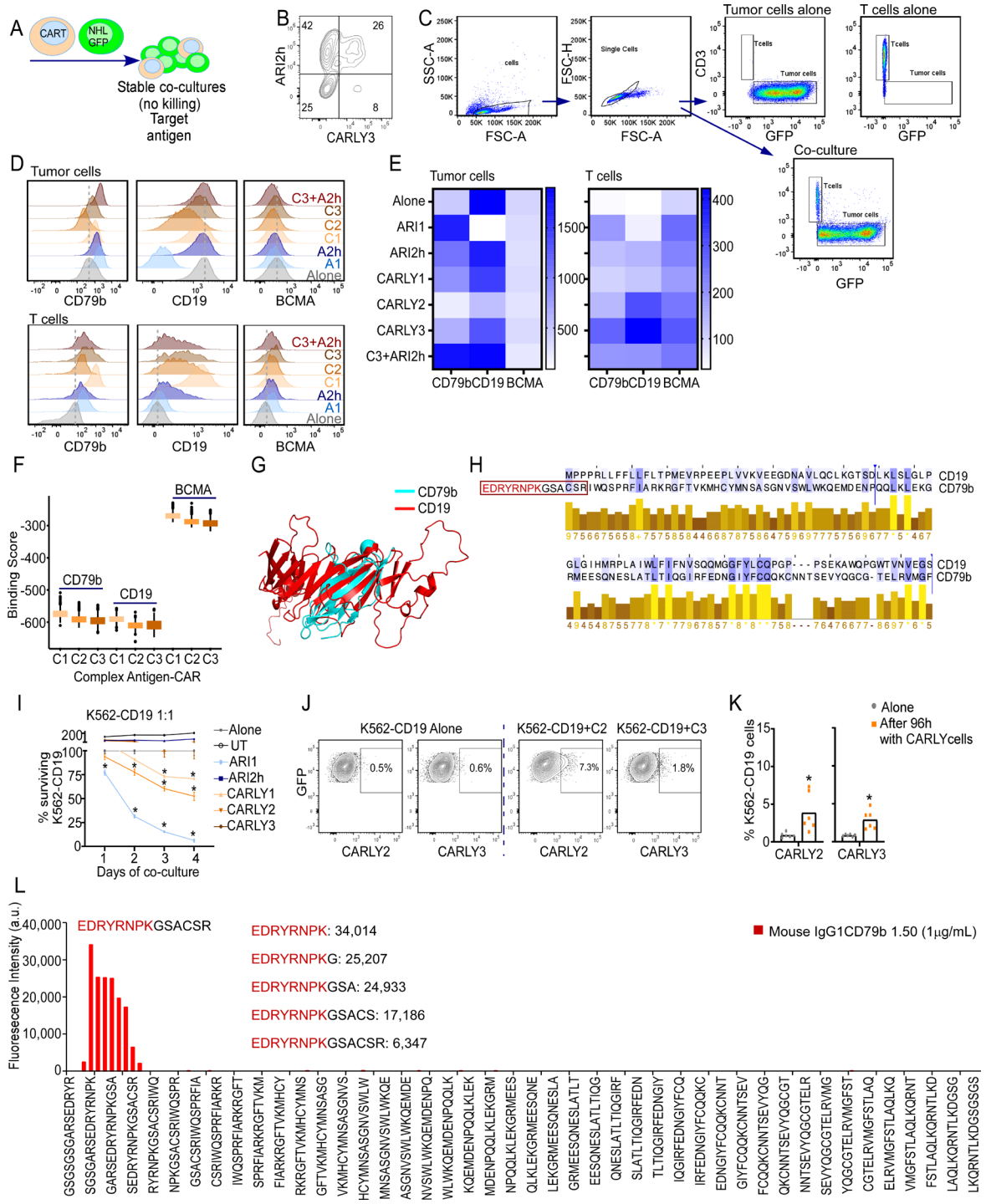

Figure 6 Loss of expression of the target antigen in NHL cells with CARLY cells and antigen recognition by CARLY cells: (A) CAR-T cells were exposed to Ramos-NHL cells in long-term cultures in conditions where CAR-T cells did not finish killing tumor cells. At this point, the target antigen was analyzed (C–E). B) Transduction efficiency for a dual CAR based on co-transduction with CARLY3 and ARI2h. (C–E) Gating strategy (C) to differentiate either T cells or tumor cells in the different conditions to analyze the target antigen (D–E). Heat map plots in (E) are performed with values obtained in (D, F). Box plot distribution of the predicted binding energy for the different CARLY1,2,3 with CD79b, CD19 and BCMA. (G) Superposition CD79b (cyan) and CD19 (red). (H) Sequence alignment derived from structural superposition in (E). Conservation degree is shown in numbers below. Additional amino acids of CD79b not aligned with CD19, which are part of the epitope mapping of CARLY2 (L) are indicated. (I) Cytotoxicity assay co-culturing K562 cells over-expressing CD19 (K562-CD19) with different T-cell subsets. (J–K) Staining of K562-CD19 cells at the end of cytotoxicity assay shown in (I) adding either CARLY2 or CARLY3. K562-CD19 were stained in the condition alone and in co-culture with either CARLY2 or CARLY3. (K) Shows six different donors of plots in (J). Epitope mapping of CARLY2 (CD79b 1.50) against CD79b showing binding intensities of CARLY2 against different peptides of CD79b. *p<0.05. See also online supplemental figure 6. BCMA, B-cell maturation antigen; CAR, chimeric antigen receptor; CARLY, CAR for Lymphoma; NHL, non-Hodgkin's lymphoma.

that ARI1 caused total CD19 loss in tumor cells. CD79b was downregulated after CARLY exposure, making this event more dramatic for CARLY2 (figure 6D–6E, online supplemental figure 6B,C), which was the CARLY showing the highest binding affinity towards CD79b (figure 2). Of interest, this loss of CD79b in CARLY2 seemed to be accompanied in some cases by a downregulation of CD19, which correlated with an increase of CD79b and CD19 in T cells, suggesting trogocytosis of both target antigens to CAR-T cells (figure 6D,E). This trogocytosis was not observed for ARI1 and CD19, as there was a complete loss of CD19 and not a downregulation. BCMA, expressed at shallow levels in resting NHL cells, did not show high variations after treatment with any CARs. Moreover, the dual CAR treatment did not induce loss of CD79b and CD19 (figure 6D,E), suggesting a possible advantage of this treatment compared with single CARs.

CARLY cells might induce phenotypic changes in tumor cells expressing CD19

To understand why CARLY cells induced concomitant loss of CD79b and CD19 and the trogocytosis observed for both antigens, we performed binding affinity predictive models analyzing the affinity of CARLY cells towards CD19, CD79b, and BCMA. Predictive models showed that, as expected, all CARLY cells had a high affinity towards CD79b and no binding affinity towards BCMA. Unexpectedly, predictive models also showed a potential binding towards CD19, with CARLY2 showing the highest one (figure 6F), which might explain the trogocytosis observed for CD19. Moreover, three-dimensional models overlapping CD19 and CD79b showed a region in both proteins with some homology (figure 6G) and highly conserved amino acid (figure 6H). To confirm whether this predicted affinity of CARLY cells towards CD19 could mediate cytotoxicity through CD19 recognition, we modified K562 myeloid cells to express CD19 (K562-CD19) as the only B-cell antigen. As expected, K562-CD19 were killed by ARI1 cells and, surprisingly, at a much lower degree by CARLY1 and CARLY2 (figure 6I). CARLY3 mediated no killing. At the end of this assay, we analyzed whether CARLY2 and 3 Abs could recognize K562-CD19 cells, to try to explain the low cytotoxicity observed with CARLY2. Flow cytometry staining showed that CARLY2 and 3 Abs did not recognize K562-CD19 cells alone, in basal conditions, and other stable transfectants overexpressing CD19 (online supplemental figure 6D,E). However, after co-culture with CARLY2 and CARLY3 cells, K562-CD19 cells were recognized at a low degree by CARLY2 and CARLY3 Abs, and not by UT T cells (figure 6J,K, and online supplemental figure 6E).

To find out the mechanisms involved in the loss of CD19 and the low degree of cytotoxicity mediated by CARLY cells through CD19 was due to a cross-reaction of the CARLY Abs towards CD19, we performed epitope mapping of CARLY2 (mouse monoclonal IgG1 CD79b.1.50) against CD79b. CARLY2 was selected for the epitope mapping as it was the one with the highest affinity towards CD79b (figure 2). Epitope mapping showed a clear and strong monoclonal Ab response against the peptide EDRYRNPK (figure 6L). This peptide was located just before the overlapping CD19 and CD79b sequences shown in predictive models disregarding the possibility of a cross-reaction of CARLY2 Ab towards CD19 (figure 6H). Therefore, this could not explain the in vitro downregulation of CD19, and cytotoxicity observed through CD19 mediated by CARLY2. Hence, different mechanisms involved in these phenomena observed will be analyzed in further studies.

NHL treatment based on dual targeting of CD79b and BCMA represents an advantage over single targeting with CARLY cells

Our previous results showed that CARLY cells might cause downregulation of the target antigen, which was not observed in vitro using a dual treatment based on CARLY3 and ARI2h. Previous studies have shown that treatment based on dual CARs obtained by co-transduction with two antigens (CD19 and CD22) represents an advantage in patients in terms of efficacy and avoiding relapses due to antigen-negative escape, and it is more economical than a treatment based on a cocktail of CARs targeting two antigens.[36 37] Therefore, in our model, as proof of principle, we compared in vivo in an advanced tumor model our best CARLY treatments (CARLY2 and 3) with a therapy based on co-transduction with CARLY3 and ARI2h. For the co-transduction CARLY3 was selected as it showed slightly superior efficacy in our in vivo studies. In this model, mice received a double dose of tumor cells, compared with previous in vivo studies, and were treated 2 days later with CAR-T cells to create an advanced tumor model (figure 7A). The dual CAR showed that in the total of transduced T cells, 27% had acquired equally both CARs, 48.8% only ARI2h, and 5.2% only CARLY3 (figure 7B). In this high tumor burden model, CARLY2 was inferior to CARLY3, and the dual CAR treatment (figure 7C,D) showed the highest survival rate (figure 7E). Analysis of tumor cells in mice tissues at the final point showed that the dual CAR treatment had the lowest number of tumor cells in BM and spleen (figure 7F). In this high tumor burden model, no loss of the target antigen was observed (figure 7G). Moreover, analysis of T cells in mice tissues demonstrated a higher persistence of CD4 T cells in BM in the dual CAR treatment group (figure 7G) and that this group had a higher percentage of CAR+T cells in the T-cell subset (figure 7I).

DISCUSSION

CAR-T cell therapy has modified the treatment concept in hematological B-cell malignancies, demonstrating superiority to the SOC in NHL[7] and representing an unprecedented advance in treating B-cell malignancies. However, still, a proportion of patients relapse after CART-19 therapy due to loss of CD19 in tumor cells.[1] Dual targeting of CD19 with CD20 or CD22 using different approaches has decreased the proportion of relapses with loss of the

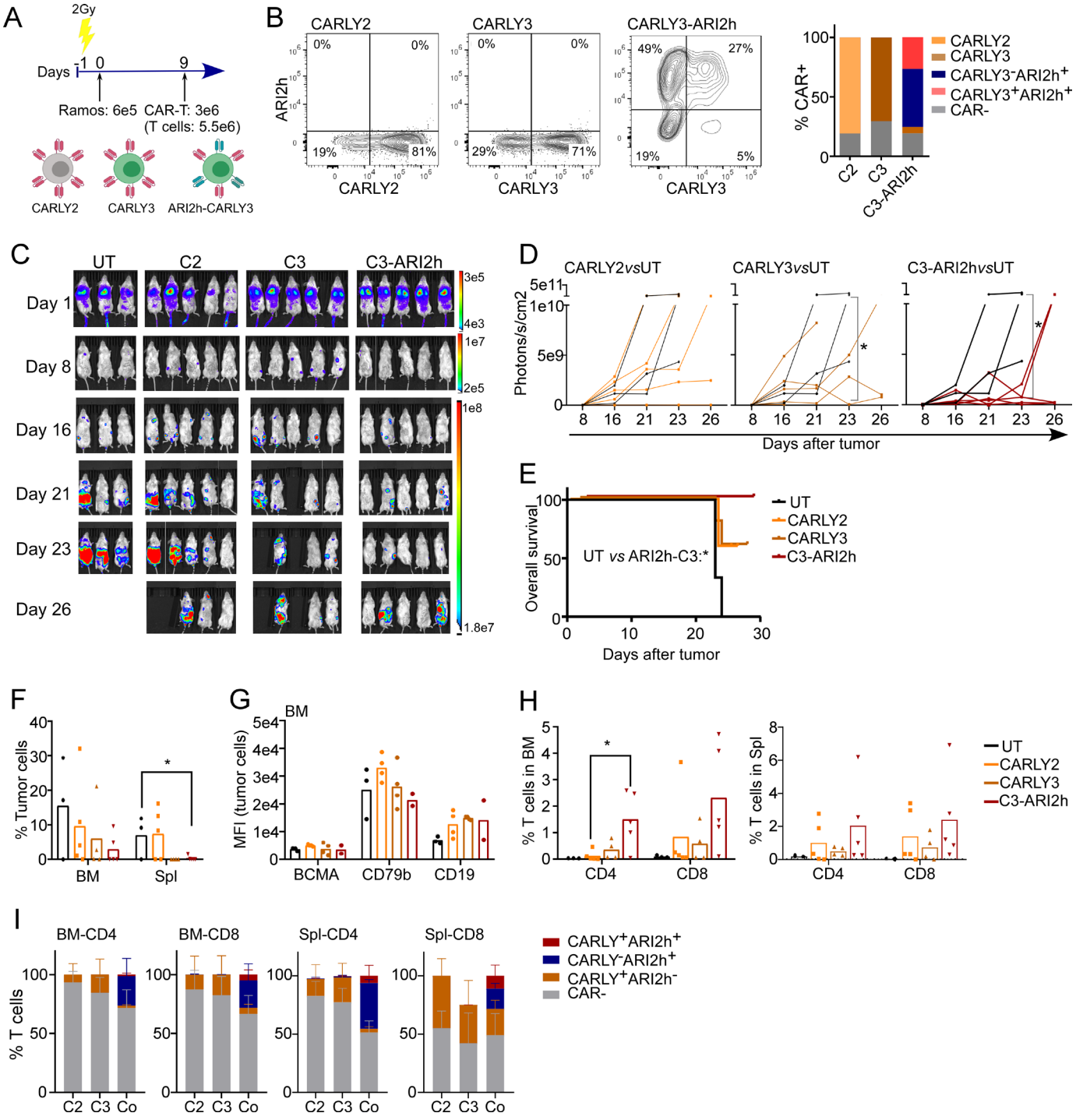

Figure 7 In vivo efficacy in a high tumor burden non-Hodgkin's lymphoma model of CARLY2 and 3 compared with a dual CAR treatment based on co-transduction of ARI2h and CARLY3. (A) Timing and doses of cells that mice received. (B) Percentage CAR+T cells in the different groups before treatment showing the two CAR$^+$ populations in the co-transduction (ARI2h-CARLY3) group. All mice received the same total number of CAR+T cells. (C–D) Disease progression is followed weekly by bioluminescence. (D) Represents numerical luminescence values of images in (C, E). Mice survival of the different groups. (F–G) Percentage of tumor cells (F) and of MFI values (G) of the target antigen (BCMA-CD79b and CD19) in tumor cells at the final point. (H) Percentage of T cells in bone marrow (BM) and spleen (Spl) at final point. (I) Percentage of CAR$^+$ T cells at final point in the different groups of mice treated with CARLY2 (C2), CARLY3 (C3) or the co-transduction (Co). *p<0.05 compared with UT T cells. BCMA. B-cell maturation antigen; CAR, chimeric antigen receptor; CARLY, CAR for Lymphoma; MFI: Median Fluroescence Intensity; UT, untransduced.

target antigen.[17–19] However, still, CARs directed at CD19 and CD20 have caused the loss of both antigens,[17] indicating that specific antigens are more prone to disappear than others, such as BCMA, whose loss in patients with MM is hardly observed.[22] Therefore, we aimed to design a CAR-T treatment for NHL based on CD79b targeting

that could avoid the loss of expression of the target antigen and would present at least the same efficacy as CARs directed to CD19 (ARI1) or BCMA (ARI2h) that are already being administered to patients with NHL and MM.[22 38] Here, we report the preclinical development of three novel CARs directed to CD79b, termed CARLY1, 2 and 3, and the analysis of their efficacy compared with CART19 and CARTBCMA cells in NHL models and also in NHL models with loss of CD19. We analyze the target antigen's loss and evaluate a possible advantage of a dual CAR treatment based on CD79b and BCMA targeting. Our results show that among the three CARLYs, CARLY3 might represent the best strategy. Moreover, we confirm a downregulation of CD79b and CD19 with concomitant trogocytosis to T cells, which is more notorious for CARLY2, the CAR with the highest binding affinity. Finally, we demonstrate that a dual CAR treatment based on co-transduction with CARLY3 and ARI2h could represent an alternative to avoid losing the target antigen.

A desirable CAR treatment should have the lowest toxicity, avoid loss of the target antigen, and persist enough to prevent relapses. In detail, CAR toxicities known as cytokine release syndrome and neurotoxicity are initiated by a massive release of cytokines by macrophages after being activated by CAR-T cells, where IL-1β and TNF-α production are highly relevant.[39 40] Moreover, on-target off-tumor toxicities can occur due to the recognition of the target antigen in other healthy tissues. In our study, CARLY2 and CARLY3 demonstrated high specificity, being even more specific against NHL than commercial CD79b Abs, and they did not recognize other tissues without B cells, suggesting that the only off-tumor toxicity developed will be B-cell aplasia. We also noticed that CARLY3 presented slower kinetics for IL-1β and TNF-α production, as their production started later than for the other CARs but continued to rise at later time points. Further studies at longer time points will clarify whether CARLY3 might have a higher proinflammatory profile than the other CARs or if it just has slower kinetics.

As previously mentioned, CAR-T cells should persist long enough to avoid relapses. Indeed, limited in vivo persistence of CAR-T cells correlates with higher relapse rates and lower PFS.[10] In this regard, CAR-T cell manufacturing involves T-cell differentiation of naïve and SCM T cells towards terminal stages. A final product as fit as possible with no highly differentiated T cells and non-senescent T cells[35] will confer higher longevity and persistence to CAR-T cells. Indeed, PI3K inhibitors added during CAR-T cell manufacturing avoid CAR-T cell differentiation and entering into senescence states, leading to more prolonged patient responses.[41] High levels of immune checkpoint markers also correlate with poorer responses after CAR-T treatment.[42] Indeed, in patients with R/R DLBCL receiving tandem CD19/CD20 CAR-T cells, a higher proportion of CD8 SCM CAR-T cells and lower LAG-3 expression were crucial for achieving durable clinical responses.[43] Moreover, LAG-3, highly expressed by exhausted T cells, presents a unique expression pattern in DLBCL, where its lowest expression clusters with genes related to T-cell activity.[44] Characterization of our CARLY products after manufacturing and compared with ARI1 and ARI2h showed that, as expected, T cells differentiated during the manufacturing and that CARLY1 showed the highest loss of naïve/SCM T cells during the expansion and the highest expression of LAG-3, suggesting a more differentiated and exhausted product that will have more limited persistence compared with CARLY2 and CARLY3 as our in vivo studies confirmed.

Additional factors that modulate CAR persistence include the hinge, transmembrane and co-stimulatory CAR domains. CARs with CD28 hinge, transmembrane domains and co-stimulatory domains induce higher tonic signaling than CD8-hinge and transmembrane-based CARs and 4-1BB co-stimulatory domains,[45] which eventually leads to apoptosis-induced cell death and early CAR disappearance.[46] Unlike other recently developed CART79b cells,[47] our CARs were designed with CD8a and 4-1BB to avoid early CAR-T cell disappearance. Antigen density and the binding affinity of the CAR also modulate CAR-T cell activity,[15] where high target antigen densities cause tonic signaling in high-affinity CARs, leading to apoptosis-induced cell death and CAR disappearance.[48] Indeed, CD79b is expressed at high levels in NHL, and CARLY2, with higher binding affinity than CARLY3, performed in vivo worse than CARLY3.

Finally, loss of CD19 is a common mechanism of relapse after CART19 in patients with NHL.[1] Some antigens are less prone to disappear, such as BCMA in MM.[6 22] In NHL, dual targeting of CD19 and CD20 with bispecific CAR-T cells caused the loss of both antigens in relapsed patients, with no loss of single antigens observed,[17] and dual targeting of CD19 and CD22 (NCT03233854) caused relapses with single loss of CD19 and not CD22. Here, CARLY cells caused downregulation of CD79b. Unlike CART19 and CD19, a total loss was not observed; instead, CD79b was trogocytosed to T cells, an event described for CART19[49] and CARTBCMA,[27] which is more characteristic of high-affinity CARs,[50] being in concordance with the higher loss and trogocytosis of CD79b observed for CARLY2, the CAR with highest binding affinity. Surprisingly, concomitant downregulation and trogocytosis of CD19 were observed, which was not an impediment for CARLY cells to eliminate NHL cells in a model of CD19-relapse. Moreover, CARLY2 could mediate some alloreactivity through CD19 recognition. However, further studies will clarify this event. Finally, to avoid downregulation of the target antigens, as proof of principle, we designed dual CAR-T cells targeting CD79b and BCMA by doing T cell co-transduction with two CARs. This dual CAR treatment avoided target antigen loss and represented the treatment with the highest efficacy.

In summary, our data suggests that CARLY3 represents a potential novel CAR treatment for NHL based on its high specificity towards NHL cells, its high in vivo efficacy, and because, compared with CARLY2, it caused a lower degree of downregulation of the target antigen.

Moreover, we plan to perform a clinical trial with CARLY3 in NHL. Once the safety of CARLY3 is demonstrated in patients, a future application of a dual CAR based on CD79b and BCMA targeting is guaranteed.

Author affiliations
[1]Department of Experimental Hematology, Health Research Institute of the Jimenez Diaz Foundation, UAM, Madrid, Spain, UAM, Madrid, Spain
[2]Next Generation CART MAD Consortium, Madrid, Spain
[3]Departamento de Desarrollo de Medicamentos de Terapias Avanzadas, Instituto de Salud Carlos III, Madrid, Spain
[4]Department of Immunology, Instituto de Investigación Sanitaria Fundación Jiménez Díaz, UAM, Madrid, Spain
[5]Department of Biomedical Science, University of Barcelona Faculty of Medicine and Health Sciences, Barcelona, Spain
[6]Josep Carreras Leukaemia Research Institute, Barcelona, Spain
[7]Hospital Clínic de Barcelona, IDIBAPS, Universidad de Barcelona, Barcelona, Spain

X Beatriz Martin-Antonio @Beatriz15995013

Acknowledgements We acknowledge personnel of the animal facility at Fundación Jiménez Diaz.

Contributors BM-A, the corresponding author, is the guarantor. Conceptualization and experiment designs: BM-A. In vitro studies of the efficacy of CARs: EE, AM-S, VS, DS-C, VP-B, and BM-A. In vivo studies of the efficacy of CARs: EE, AM-S, DS-C, and BM-A. Optimization and analysis in paraffin-embedded tissue samples: JS-L and JB. Stable cell lines overexpressing CD19: JF-C and EE. Predictive models: NF-F. Production of monoclonal antibodies, Epitope Mapping: PE. Funding: LS-B, PL-S, and BM-A. Analysis of results: AM-S, VS, and BM-A. Manuscript writing: BM-A. All authors have reviewed and approved the final version of this manuscript.

Funding This work has been supported by grants from "Instituto de Salud Carlos III", Spanish Ministry of Health (co-founded by the EU) (grants: PI20/00991, CP21/0011), by a grant from "Dirección General de Investigación e Innovación Tecnológica" of the Community of Madrid (grant: S2022/BMD-7225), by the "Asociación Madrileña de Hematologia (grant: PR0000002635) and by funds of the CARIBE project. BMA is supported by the Miguel Servet Program of ISCIII (CP21/00111).

Competing interests BM-A and MJ have a patent for ARI0002h cells. BM-A, LS-B, JS-L and PL-S have the patent for CARLY cells.

Patient consent for publication Not applicable.

Ethics approval Research involving human materials was approved by the Clinical Research Ethical Committee (Fundación Jiménez Diaz, Madrid, Spain). All animal work was performed with approval from the Animal Research Ethical Committee (Fundación Jiménez Diaz, Madrid, Spain).

Provenance and peer review Not commissioned; externally peer reviewed.

Data availability statement All data relevant to the study are included in the article or uploaded as supplementary information.

ORCID iDs
Manel Juan http://orcid.org/0000-0002-3064-1648
Beatriz Martin-Antonio http://orcid.org/0000-0003-0612-2693

REFERENCES

1 Neelapu SS, Locke FL, Bartlett NL, *et al*. Axicabtagene Ciloleucel CAR T-Cell Therapy in Refractory Large B-Cell Lymphoma. *N Engl J Med* 2017;377:2531–44.
2 Abramson JS, Palomba ML, Gordon LI, *et al*. Pivotal Safety and Efficacy Results from Transcend NHL 001, a Multicenter Phase 1 Study of Lisocabtagene Maraleucel (liso-cel) in Relapsed/Refractory (R/R) Large B Cell Lymphomas. *Blood* 2019;134:241.
3 Maude SL, Laetsch TW, Buechner J, *et al*. Tisagenlecleucel in Children and Young Adults with B-Cell Lymphoblastic Leukemia. *N Engl J Med* 2018;378:439–48.
4 San-Miguel J, Dhakal B, Yong K, *et al*. Cilta-cel or Standard Care in Lenalidomide-Refractory Multiple Myeloma. *N Engl J Med* 2023;389:335–47.
5 Munshi NC, Anderson LD Jr, Shah N, *et al*. Idecabtagene Vicleucel in Relapsed and Refractory Multiple Myeloma. *N Engl J Med* 2021;384:705–16.
6 Berdeja JG, Madduri D, Usmani SZ, *et al*. Ciltacabtagene autoleucel, a B-cell maturation antigen-directed chimeric antigen receptor T-cell therapy in patients with relapsed or refractory multiple myeloma (CARTITUDE-1): a phase 1b/2 open-label study. *The Lancet* 2021;398:314–24.
7 Locke FL, Miklos DB, Jacobson CA, *et al*. Axicabtagene Ciloleucel as Second-Line Therapy for Large B-Cell Lymphoma. *N Engl J Med* 2022;386:640–54.
8 Westin JR, Locke FL, Dickinson M, *et al*. n.d. Data from Safety and Efficacy of Axicabtagene Ciloleucel versus Standard of Care in Patients 65 Years of Age or Older with Relapsed/Refractory Large B-Cell Lymphoma.
9 Abramson JS, Solomon SR, Arnason J, *et al*. Lisocabtagene maraleucel as second-line therapy for large B-cell lymphoma: primary analysis of the phase 3 TRANSFORM study. *Blood* 2023;141:1675–84.
10 Jackson Z, Hong C, Schauner R, *et al*. Sequential Single-Cell Transcriptional and Protein Marker Profiling Reveals TIGIT as a Marker of CD19 CAR-T Cell Dysfunction in Patients with Non-Hodgkin Lymphoma. *Cancer Discov* 2022;12:1886–903.
11 Kim W, Kim SJ, Yoon DH, *et al*. PHASE 2 STUDY OF ANBAL-CEL, NOVEL ANTI-CD19 CAR-T THERAPY WITH DUAL SILENCING OF PD-1 AND TIGIT IN RELAPSED OR REFRACTORY LARGE B CELL LYMPHOMA - INTERIM ANALYSIS RESULT. *Hematol Oncol* 2023;41:81–2.
12 Yan Z-X, Li L, Wang W, *et al*. Clinical Efficacy and Tumor Microenvironment Influence in a Dose-Escalation Study of Anti-CD19 Chimeric Antigen Receptor T Cells in Refractory B-Cell Non-Hodgkin's Lymphoma. *Clin Cancer Res* 2019;25:6995–7003.
13 Jin J, Lin L, Meng J, *et al*. High-multiplex single-cell imaging analysis reveals tumor immune contexture associated with clinical outcomes after CAR T cell therapy. *Mol Ther* 2024;32:1252–65.
14 Jacoby E, Nguyen SM, Fountaine TJ, *et al*. CD19 CAR immune pressure induces B-precursor acute lymphoblastic leukaemia lineage switch exposing inherent leukaemic plasticity. *Nat Commun* 2016;7:12320.
15 Majzner RG, Rietberg SP, Sotillo E, *et al*. Tuning the Antigen Density Requirement for CAR T-cell Activity. *Cancer Discov* 2020;10:702–23.
16 Du J, Zhang Y. Sequential anti-CD19, 22, and 20 autologous chimeric antigen receptor T-cell (CAR-T) treatments of a child with relapsed refractory Burkitt lymphoma: a case report and literature review. *J Cancer Res Clin Oncol* 2020;146:1575–82.
17 Zhang Y, Wang Y, Liu Y, *et al*. Long-term activity of tandem CD19/CD20 CAR therapy in refractory/relapsed B-cell lymphoma: a single-arm, phase 1-2 trial. *Leukemia* 2022;36:189–96.
18 Larson SM, Walthers CM, Ji B, *et al*. CD19/CD20 Bispecific Chimeric Antigen Receptor (CAR) in Naive/Memory T Cells for the Treatment of Relapsed or Refractory Non-Hodgkin Lymphoma. *Cancer Discov* 2023;13:580–97.
19 Shah NN, Johnson BD, Schneider D, *et al*. Bispecific anti-CD20, anti-CD19 CAR T cells for relapsed B cell malignancies: a phase 1 dose escalation and expansion trial. *Nat Med* 2020;26:1569–75.
20 Spiegel JY, Patel S, Muffly L, *et al*. CAR T cells with dual targeting of CD19 and CD22 in adult patients with recurrent or refractory B cell malignancies: a phase 1 trial. *Nat Med* 2021;27:1419–31.
21 Shalabi H, Qin H, Su A, *et al*. CD19/22 CAR T cells in children and young adults with B-ALL: phase 1 results and development of a novel bicistronic CAR. *Blood* 2022;140:451–63.
22 Oliver-Caldés A, González-Calle V, Cabañas V, *et al*. Fractionated initial infusion and booster dose of ARI0002h, a humanised, BCMA-directed CAR T-cell therapy, for patients with relapsed or refractory multiple myeloma (CARTBCMA-HCB-01): a single-arm, multicentre, academic pilot study. *Lancet Oncol* 2023;24:913–24.

23 Bluhm J, Kieback E, Marino SF, *et al*. CAR T Cells with Enhanced Sensitivity to B Cell Maturation Antigen for the Targeting of B Cell Non-Hodgkin's Lymphoma and Multiple Myeloma. *Mol Ther* 2018;26:1906–20.
24 Tilly H, Morschhauser F, Sehn LH, *et al*. Polatuzumab Vedotin in Previously Untreated Diffuse Large B-Cell Lymphoma. *N Engl J Med* 2022;386:351–63.
25 Gouni S, Rosenthal AC, Crombie JL, *et al*. A multicenter retrospective study of polatuzumab vedotin in patients with large B-cell lymphoma after CAR T-cell therapy. *Blood Adv* 2022;6:2757–62.
26 Castella M, Boronat A, Martín-Ibáñez R, *et al*. Development of a Novel Anti-CD19 Chimeric Antigen Receptor: A Paradigm for an Affordable CAR T Cell Production at Academic Institutions. *Mol Ther Methods Clin Dev* 2019;12:134–44.
27 Perez-Amill L, Suñe G, Antoñana-Vildosola A, *et al*. Preclinical development of a humanized chimeric antigen receptor against B cell maturation antigen for multiple myeloma. *Haematologica* 2021;106:173–84.
28 Su Q, Chen M, Shi Y, *et al*. Cryo-EM structure of the human IgM B cell receptor. *Science* 2022;377:875–80.
29 Rose PW, Beran B, Bi C, *et al*. The RCSB Protein Data Bank: redesigned web site and web services. *Nucleic Acids Res* 2011;39:D392–401.
30 Lefranc M-P, Pommié C, Ruiz M, *et al*. IMGT unique numbering for immunoglobulin and T cell receptor variable domains and Ig superfamily V-like domains. *Dev Comp Immunol* 2003;27:55–77.
31 Fernandez-Fuentes N, Rai BK, Madrid-Aliste CJ, *et al*. Comparative protein structure modeling by combining multiple templates and optimizing sequence-to-structure alignments. *Bioinformatics* 2007;23:2558–65.
32 Schneidman-Duhovny D, Inbar Y, Nussinov R, *et al*. PatchDock and SymmDock: servers for rigid and symmetric docking. *Nucleic Acids Res* 2005;33:W363–7.
33 Sircar A, Gray JJ. SnugDock: paratope structural optimization during antibody-antigen docking compensates for errors in antibody homology models. *PLoS Comput Biol* 2010;6:e1000644.
34 Leaver-Fay A, Tyka M, Lewis SM, *et al*. ROSETTA3: an object-oriented software suite for the simulation and design of macromolecules. *Methods Enzymol* 2011;487:545–74.
35 Battram AM, Bachiller M, Martín-Antonio B. Senescence in the Development and Response to Cancer with Immunotherapy: A Double-Edged Sword. *Int J Mol Sci* 2020;21:4346.
36 Kokalaki E, Ma B, Ferrari M, *et al*. Dual targeting of CD19 and CD22 against B-ALL using a novel high-sensitivity aCD22 CAR. *Mol Ther* 2023;31:2089–104.
37 Ghorashian S, Lucchini G, Richardson R, *et al*. CD19/CD22 targeting with cotransduced CAR T cells to prevent antigen-negative relapse after CAR T-cell therapy for B-cell ALL. *Blood* 2024;143:118–23.
38 Ortíz-Maldonado V, Rives S, Castellà M, *et al*. CART19-BE-01: A Multicenter Trial of ARI-0001 Cell Therapy in Patients with CD19$^+$ Relapsed/Refractory Malignancies. *Mol Ther* 2021;29:636–44.
39 Ye L, Huang Y, Zhao L, *et al*. IL-1β and TNF-α induce neurotoxicity through glutamate production: a potential role for neuronal glutaminase. *J Neurochem* 2013;125:897–908.
40 Norelli M, Camisa B, Barbiera G, *et al*. Monocyte-derived IL-1 and IL-6 are differentially required for cytokine-release syndrome and neurotoxicity due to CAR T cells. *Nat Med* 2018;24:739–48.
41 Raje NS, Shah N, Jagannath S, *et al*. Updated Clinical and Correlative Results from the Phase I CRB-402 Study of the BCMA-Targeted CAR T Cell Therapy bb21217 in Patients with Relapsed and Refractory Multiple Myeloma. *Blood* 2021;138:548.
42 Oliver-Caldes A, Español-Rego M, Zabaleta A, *et al*. Biomarkers of Efficacy and Safety of the Academic BCMA-CART ARI0002h for the Treatment of Refractory Multiple Myeloma. *Clin Cancer Res* 2024;30:2085–96.
43 Wang Y, Tong C, Lu Y, *et al*. Characteristics of premanufacture CD8+ T cells determine CAR-T efficacy in patients with diffuse large B-cell lymphoma. *Sig Transduct Target Ther* 2023;8:1–11.
44 Lee H, Yoon SE, Kim SJ, *et al*. A unique expression pattern of LAG3 distinct from that of other immune checkpoints in diffuse large B-cell lymphoma. *Cancer Med* 2023;12:16359–69.
45 Alabanza L, Pegues M, Geldres C, *et al*. Function of Novel Anti-CD19 Chimeric Antigen Receptors with Human Variable Regions Is Affected by Hinge and Transmembrane Domains. *Mol Ther* 2017;25:2452–65.
46 Caruso HG, Hurton LV, Najjar A, *et al*. Tuning Sensitivity of CAR to EGFR Density Limits Recognition of Normal Tissue While Maintaining Potent Antitumor Activity. *Cancer Res* 2015;75:3505–18.
47 Chu F, Cao J, Liu J, *et al*. Chimeric antigen receptor T cells to target CD79b in B-cell lymphomas. *J Immunother Cancer* 2023;11:e007515.
48 Calderon H, Mamonkin M, Guedan S. Analysis of car-mediated tonic signaling. In: Swiech K, Malmegrim KCR, Picanço-Castro V, eds. *Chimeric Antigen Receptor T Cells: Development and Production*. New York, NY: Springer US, 2020: 223–36. Available: https://doi.org/10.1007/978-1-0716-0146-4_17
49 Hamieh M, Dobrin A, Cabriolu A, *et al*. CAR T cell trogocytosis and cooperative killing regulate tumour antigen escape. *Nature New Biol* 2019;568:112–6.
50 Olson ML, Mause ERV, Radhakrishnan SV, *et al*. Low-affinity CAR T cells exhibit reduced trogocytosis, preventing rapid antigen loss, and increasing CAR T cell expansion. *Leukemia* 2022;36:1943–6.